

See discussions, stats, and author profiles for this publication at: <https://www.researchgate.net/publication/327870890>

Autonomic Transmission Through pre-FEC BER Degradation Prediction Based on SOP Monitoring

Conference Paper · September 2018

CITATIONS

0

READS

46

5 authors, including:



Behnam Shariati

Universitat Politècnica de Catalunya

36 PUBLICATIONS 169 CITATIONS

SEE PROFILE



Marc Ruiz

Universitat Politècnica de Catalunya

114 PUBLICATIONS 932 CITATIONS

SEE PROFILE



Luis Velasco Esteban

Universitat Politècnica de Catalunya

229 PUBLICATIONS 1,777 CITATIONS

SEE PROFILE

Some of the authors of this publication are also working on these related projects:



METRO High bandwidth, 5G Application-aware optical network, with edge storage, compUte and low Latency (METRO-HAUL) [View project](#)



Metro-Haul: METRO High bandwidth, 5G Application-aware optical network, with edge storage, compUte and low Latency [View project](#)

Autonomic Transmission Through pre-FEC BER Degradation Prediction Based on SOP Monitoring

B. Shariati ⁽¹⁾, F. Boitier ⁽²⁾, M. Ruiz ⁽¹⁾, P. Layec ⁽²⁾, and L. Velasco ^{(1)*}

⁽¹⁾ Universitat Politècnica de Catalunya, Barcelona, Spain, *lvelasco@ac.upc.edu

⁽²⁾ Nokia Bell Labs, Nozay, France

Abstract An *Autonomic Transmission Agent* based on machine-learning is proposed for excessive bit-error-rate prediction resulting from real-time analysis of state-of-polarization (SOP). The accuracy and speed of the agent enables its use for local and remote transceiver reconfiguration.

Introduction

As the coherent technology is introduced in metro networks, energy and cost constraints become predominant¹. A solution is to reduce the number of bits of analog-to-digital converters (ADCs), which are mandatory for coherent technology, to only 4-5 bits instead of 8 bits typically used in long haul networks. This causes a penalty in terms of performance² and, thus, the resulting bit error rate (BER) previous the forward error correction (FEC) is more sensitive to physical fluctuations, such as the state of polarization (SOP) rotation.

Autonomic transmission, enabled by monitoring and machine learning (ML) algorithms, can provide a great opportunity to lower the impact of dynamic physical layer impairments through adaptive component reconfiguration; this can be realized in the local node or in a remote node through the SDN controller, allowing very quick reaction to changes and resolving issues that may affect the quality of transmission (QoT).

This paper proposes an autonomic transmission solution, as an extension for current coherent based transceivers, focuses on anticipating pre-FEC BER degradation of individual lightpaths by monitoring in real time the Stokes parameters representing the SOP. Note that SOP monitoring coupled with ML has been already demonstrated for fiber break prediction³. In this work, we target two alternative use-cases where the SOP is monitored: *i)* the anticipation of BER degradation can trigger a reconfiguration of the local receiver by increasing the number of FEC decoding iterations; *ii)* the remote transmitter can also be reconfigured by changing, e.g., the FEC coding rate, modulation format or baud-rate. While the local reconfiguration usually takes short times, BER degradation can be anticipated just few milliseconds ahead. In contrast, remote reconfiguration requires longer times since it entails control plane messages, so BER degradation needs to be anticipated with more time, e.g., 100ms.

Autonomic transmission

Automating the optical transport layer is a key enabler for the sustainable growth of the networks, due in part to the increase in the

dynamicity and complexity of the networks. In fact, network-wide performance can be substantially enhanced while reducing the margins and minimizing the human intervention. Targeting the above, we propose an *Autonomic Transmission Agent* (ATA) to lower the impact of physical layer degradations. Considering a point-to-point connection shown in Fig. 1, the ATA receives monitoring data from the receiver (labelled 1), analyzes the data, and provides guidelines and operational decisions for the local receiver (2a) or the remote transmitter through the node controller (2b). Sophisticated ML tools are key building blocks of the ATA.

SOP-based pre-FEC BER prediction

In this section, we present a set of algorithms for the ATA that continuously receives SOP monitored by the receiver and provides short-term and long-term BER predictions. Short and long-term predictions can be interpreted as two complementary phases of prediction. In the first phase (for the next tens of ms), the algorithm estimates the BER after crossing a certain threshold. In the second phase (for the next hundreds of ms), the algorithm provides a long-term anticipation of the evolution of BER.

Fig. 2 plots the evolution of the Stokes parameters and the BER for a case where an unexpected event affecting the proper transmission of a lightpath occurs at time t_0 (see³ for more examples). Both SOP and BER

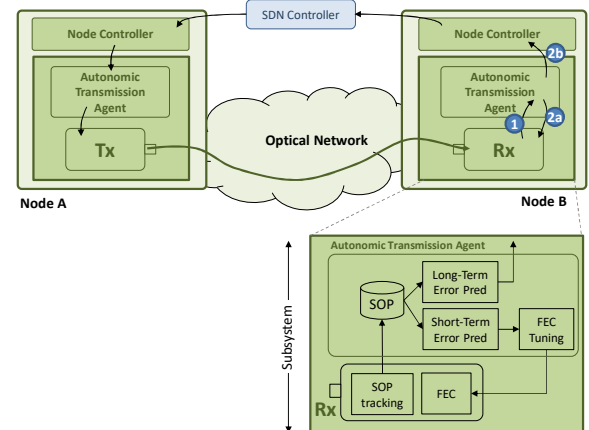


Fig. 1: Autonomic transmission and detail of receiver side

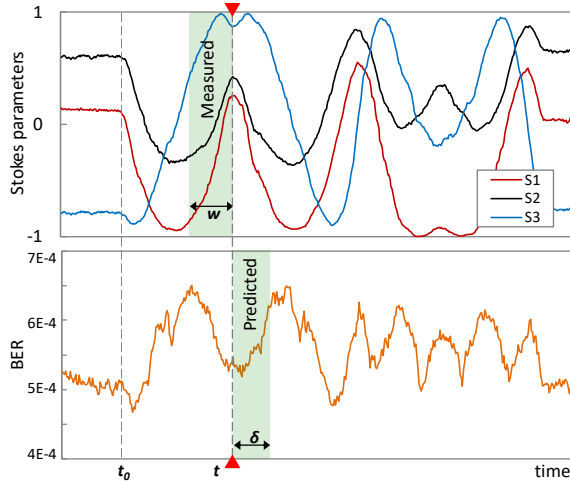


Fig. 2: SOP-based pre-FEC BER prediction

start fluctuating after t_0 , revealing some correlation between them. In view of that correlation, we propose a predictive model that can be used at any time t to forecast the expected BER for a given future time $t+\delta$ based on the SOP data measured in the past time window $[t-w, t]$. The model can be used for both long and short-term BER prediction by training it with the proper δ for the targeted prediction.

The predictive model, based on the naïve Bayes approach⁴, aims at mapping the SOP evolution within the time window $[t-w, t]$ with the probability that the BER takes a given value at time $t+\delta$. In practice, the model can be implemented as a hash table, where each key encodes a specific SOP evolution pattern and contains a vector of probabilities of all the BER values observed for that SOP evolution.

The advantage of this probabilistic model is three-fold: *i)* it allows considering any possible complex correlation between SOP and BER, without any prior assumption on that; *ii)* using probabilities increases its flexibility for different cases. For short-term prediction, a simple weighted average BER can be obtained as a good BER estimator. However, since large δ impact negatively on accuracy, the probability that BER exceeds a given threshold becomes a more robust prediction outcome; and *iii)* its computational cost is almost negligible, which allows very fast operation.

The algorithm in Table I is used for model training from a dataset $D_{w\delta}$ containing SOP and BER monitoring measurements for a specific pair w, δ . Let us consider that each row in $D_{w\delta}$ contains a number of Stokes values for a given window $[t-w, t]$ and the BER measured at the target time $t+\delta$. After initializing the empty model F , the training procedure starts by summarizing each row into 6 relevant features (two per Stokes parameter) related to SOP evolution: the Stokes parameters measured at time t and their trend within the window (lines 1-2 in Table 1). Those continuous values are then discretized

Table 1: Training Algorithm

INPUT:	$D_{w\delta}, p, q$
OUT:	$model_{w\delta}$
1:	$F \leftarrow \emptyset$
2:	$X_c \leftarrow \text{computeFeatures}(D_{w\delta}.\text{SOP})$
3:	$X, r_{\text{SOP}} \leftarrow \text{discretize}(X_c, p)$
4:	$Y, r_{\text{BER}} \leftarrow \text{discretize}(D_{w\delta}.\text{BER}, q)$
5:	for i in $1..\text{length}(X)$ do
6:	$\text{key} \leftarrow \text{labeling}(X[i])$
7:	if $F[\text{key}][Y[i]] == \emptyset$ then
8:	$F[\text{key}][Y[i]] \leftarrow 0$
9:	$F[\text{key}][Y[i]]++$
10:	for key in $F.\text{keys}()$ do
11:	$F[\text{key}][*] \leftarrow F[\text{key}][*] / \text{sum}(F[\text{key}][*])$
12:	return $\{F, r_{\text{SOP}}, r_{\text{BER}}\}$

into p segments of equal length (line 3). For example, for a given Stoke parameter (whose continuous range is $[-1, 1]$) and $p=20$, segment 1 will contain those rows in the range $[-1, -0.9]$, segment 2 those in the range $[-0.9, -0.8]$, and so on. Similarly, BER is also discretized into q segments of equal length (line 4). Note that discretization of SOP and BER measures returns also continuous ranges (r), which are needed to translate continuous values to segments and vice-versa.

After obtaining discrete SOP features and BER, every row is firstly mapped to a label according discrete SOP features (lines 5-6); a row whose discrete features take the values 1, 5, 13, 20, 17, and 5, is labelled as '010513201705'. Then, the count of rows of that SOP label with the BER segment is incremented (lines 7-9). This procedure ends with a table that contains the count of each SOP label and BER segment, which is easily converted into an empirical probability by dividing cell values over the sum of the rows defined by keys (lines 10-11).

Results

The accuracy of the proposed algorithms in predicting pre-FEC BER variations is evaluated in this section. The SOP and the corresponding dataset have been collected from an experimental setup that includes a QPSK optical coherent transmission, implemented on a real-time FPGA³ using a low resolution 5-bit ADC, along 50km of SMF fiber. Mechanical events are caused by a programmable robot arm twisting the fiber. SOP monitoring samples, extracted from the de-multiplexed polarization steps in the digital signal processing are gathered at a rate of 3,600 samples per second. Every experiment is triggered by rotation speed threshold and contains 2000 samples before the triggering event and 14000 samples after it. At every time interval, the number of errors is evaluated by counting the difference between the expected pseudorandom sequence and the decoded one (by step of 32 bits) on each tributary. The BER is then computed by considering the baud rate, the polarization multiplexed factor, and the QPSK number of bits.

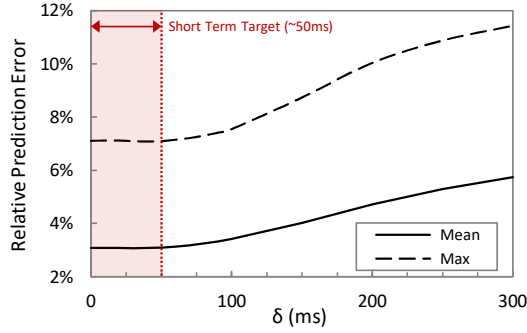


Fig. 3: Prediction accuracy

500 different experiments were carried out. Out of these experiments, we selected ~100 experiments for training and testing the proposed algorithm in which, due to mechanical stress, the BER significantly increases beyond proper operation period measurements. For the BER prediction, we use the relative prediction error (RPE), defined as $(\text{predictedBER} - \text{realBER}) / \text{realBER}$, as a metric to evaluate the prediction accuracy of the algorithm. We aim at accurately predicting those higher values of BER, i.e. when it exceeds the mean plus 3 times the standard deviation measured during the proper operation period.

The obtained results are shown in Fig. 3, where the mean and maximum values of RPE are presented for a range δ . High prediction accuracy for the 50ms short-term target is shown, with only 3% mean and about 7% of max RPE. However, the accuracy decreases as longer prediction time windows are considered. To complement the above results, Fig. 4 shows BER prediction using a model for $\delta=10\text{ms}$ for two different experiments; one can observe how algorithm accurately follows the evolution of BER, regardless of SOP fluctuations.

As the accuracy predicting the BER decreases for longer time windows, in the second phase we focus on anticipating whether the BER will exceed a particular threshold and therefore, the accuracy of the algorithm will be evaluated in terms of BER threshold violation. In order to setup this threshold, the mean and standard deviation of errors during the operation phase was computed for every experimental measurement and then, the threshold was set to the mean plus 6 times the standard deviation. We first trained the model with different w ranging from 0 to 200 ms; the obtained results are presented in terms of the threshold violation anticipation time as a function of w (Fig. 5a). In view of the results, we can conclude that $w=150\text{ms}$, i.e., last 540 SOP samples (6 kB storage), allows the best overall accuracy and allows anticipating threshold violation up to 45% times sooner than other window sizes (dashed line). These results allow validating the proposed methodology for both use cases and additionally, to highlight that different models are

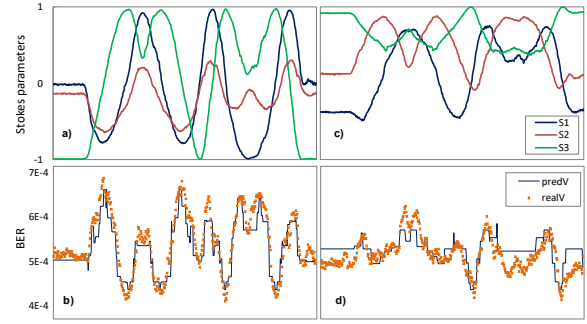


Fig. 4: BER estimations of two different SOP profiles

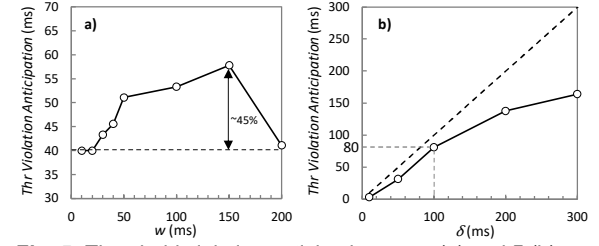


Fig. 5: Threshold violation anticipation vs. w (a) and δ (b)

needed for different prediction time scopes. With that optimum w configuration, the analysis of how long δ can be to guarantee an accurate threshold violation detection is presented in Fig. 5b, which plots the actual threshold anticipation time as a function of δ . Although models could potentially target anticipation time equal to δ (dashed line), this becomes slightly smaller since increasing δ makes it more difficult to detect threshold violation when it happens and consequently, this delays the anticipated detection. However, 80ms of actual threshold anticipation can be achieved when $\delta=100\text{ms}$. After that, detection time drops and therefore, $\delta=100\text{ms}$ is proposed for long-term models to anticipate threshold violation and trigger some reconfiguration procedure at transmitter location.

Conclusion

An autonomic transmission agent has been proposed to enhance the performance of optical transmission systems. The agent benefits from extremely low complexity, minimal storage, and speed to leave sufficient time for local and remote transceiver reconfiguration.

Acknowledgements

This research has received funding from the EC through the METRO-HAUL project (G.A. n° 761727), the AEI/FEDER TWINS project (TEC2017-90097-R), and ICREA Institution.

References

- [1] T. Kupfer *et al.*, "Optimizing Power Consumption of a Coherent DSP for Metro and Data Center Interconnects," in Proc. OFC 2017.
- [2] X. Chen *et al.*, "Experimental Quantification of Implementation Penalties from Limited ADC Resolution for Nyquist Shaped Higher-Order QAM," in Proc. ECOC, 2016.
- [3] F. Boitier *et al.*, "Proactive fiber damage detection in real-time coherent receiver," in Proc. ECOC, 2017.
- [4] Ch. Bishop, "Pattern Recognition and Machine Learning," Springer-Verlag, 2006.